

# Damage Statistics in Progressively Compressed Arrays of Nano-pillars

Zbigniew Domański

**Abstract**—Failures in arrays of nano-pillars evolve in a complicated way. When a square array, involving  $N$  pillars characterized by random pillar-load-thresholds  $\{\sigma_i\}$ ,  $1 \leq i \leq N$ , is subjected to a load  $Q$ , that crushes some weak pillars, then short sequences of failures appear. If the load is applied progressively to the array, these sequences develop in avalanches of failures, consecutive numbers of intact pillars decrease and the array approaches its limit of integrity. This limiting state of the array is characterized by the critical load  $Q_c$  and the number  $n_c < N$  of non-crushed pillars, whereas  $Q > Q_c$  induces an irreversible destruction of the array. Using computer simulations we study distributions of  $Q_c$  and  $n_c$  and we show that for arrays with pillar-load-thresholds  $\{\sigma_i\}$  taken from a Weibull distribution, the ratio  $Q_c/n_c$  is distributed according to a skew-normal distribution and the mean value  $\bar{Q}_c \sim N/(\log(N))^\delta$  with  $0 < \delta < 1$ .

**Index Terms**—array of pillars, avalanches, critical load, evolving failure, probability distribution.

## I. INTRODUCTION

ARRAYS with a large number of vertical pillars assembled on flat substrates are encountered in many areas of modern technology such as bio-chemistry, nano-scale electronics or photovoltaics [1], [2], [3], [4]. Uniaxial tension and compression testing of micro-scale metallic pillars shows a substantial strength increase due to size reduction of the pillars [4]. Under the growing load, however the pillars begin to fracture. A possible sequence of failures among pillars decreases the device performance and may trigger a catastrophic avalanche of failures. This is because an array placed under an increasing load starts to fail immediately when the internal load intensity exceeds the critical value of weakest pillars and the failure develops in a form of avalanches of simultaneously crushed pillars. More exactly, avalanches emerge when a growing load eliminates a pillar from the set of working pillars and this elimination changes the internal load pattern sufficiently to force the failure of other pillars and, in consequence, generating a wave of destruction. An efficient approach to study avalanches of failures employs load-transfer models. Specifically, the Fibre Bundle Models (FBM) and Random Fuse Models are frequently employed in a context of technological applications [5], [6], [7], [8].

In this work, the array of pillars is represented by a collection of vertical pillars located at nodes of a square lattice, see Fig. 1, and then analysed under a Fibre Bundle Model framework [9], [10], [11], [12], [13]. We limit our study to the case where each pillar can only be in one of two states: working or irreversibly crushed. In our simulations, an ensemble of  $N$  pillars is subjected to a growing load  $Q$ , that eliminates weak components and induces avalanches of

failures. This means that when a pillar breaks, its load is distributed among the other intact pillars and thus the probability of subsequent failures increases. The model hinges crucially on a load-transfer-rule. Among many different rules there are two extreme ones: global (equal) load sharing (GLS) and local load sharing (LLS) [14], [15], [16].

Fabrication errors and material imperfections influence the behaviour of pillars under load. Due to these imperfections, pillars' yields are non-homogeneous and we represent multiple pillar-failure modes by the pillar-load-thresholds. During our simulations these load-thresholds are modelled by quenched random variables governed by the Weibull distribution [17], [18].

## II. COMPUTATION METHOD

For the purpose of this study, we employ the LLS transfer rule. We opt for this rule due to the fact that a multitude of arrays of pillars have flexible supports. In consequence

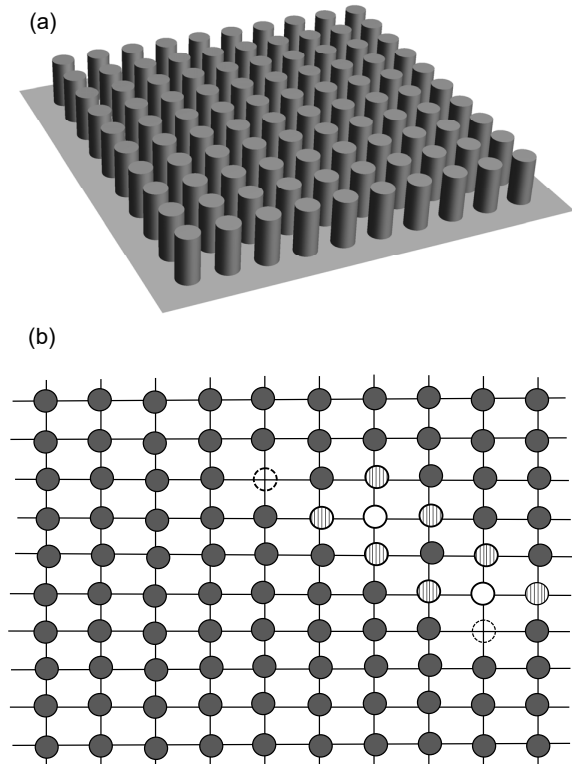


Fig. 1. An array of vertical pillars: (a) schematic view, (b) example of the LLS rule application. Disks represent pillars: black disks – working pillars, open circles – crushed pillars, white discs – just damaged pillars with their loads transferred to nearest intact pillars marked by patterned disks.

Manuscript received October 17, 20018; revised November 2, 2018.

Z. Domański is with the Institute of Mathematics, Czestochowa University of Technology, Dabrowskiego 69, PL-42201 Czestochowa, Poland. (corresponding author e-mail: zbigniew.domanski@im.pcz.pl).

during a loading process stresses accumulate in close vicinities of crushed pillars. This means that within a short interval between consecutive failures the load carried by the destroyed pillar is transferred only to its closest intact neighbours. Because of such a limited-range-load-transfer, internal loads are distributed non-uniformly and regions of load accumulation appear throughout the entire array. The increasing internal load on the intact pillars triggers other failures, after which each surviving pillar feels growing load. If the load transfer does not induce further failures, a stable pillars' configuration emerges. This means that the given value  $Q$  is not high enough to crush the entire array, and the applied load has to increase. In the simulations we apply a quasi-static loading procedure: if the system is in a stable state the applied load  $Q$  uniformly increases to  $Q + \delta Q$  until the weakest working pillar breaks.

A series of increases in the value of the external load gives  $Q = Q_c + \delta Q$  which induces an avalanche of failures among all still working pillars. Application of quasi-static loading allows us to identify a minimal load  $Q$  necessary for destruction of all the pillars and thus to get  $Q_c$  and  $n_c$  that characterize the array of pillars on the edge of its functionality.

In our simulation, pillar-strength-thresholds  $\sigma_{th}$  are taken from the Weibull distribution [19], [20]. The corresponding probability density function is given by

$$p_{k,\lambda}(\sigma_{th}) = (k/\lambda)(\sigma_{th}/\lambda)^{k-1} \exp[-(\sigma_{th}/\lambda)^k] \quad (1)$$

Parameters  $k > 0$  and  $\lambda > 0$  define the shape and scale of this density function. Shape parameter  $k$  (also called Weibull index) controls the amount of disorder in the system. Without loss of generality, we assume  $\lambda = 1$  and thus the corresponding probability density reads

$$p_k(\sigma_{th}) = p_{k,1}(\sigma_{th}) = k\sigma_{th}^{k-1} \exp[-\sigma_{th}^k] \quad (2)$$

We address a question how these pillar-load-thresholds, distributed according to (2), determine an effective-global critical load  $Q_c$  and limiting number of working pillars  $n_c$ . Due to results of our numerical simulations, we have found that coefficient of skewness of distribution of  $Q_c/n_c$  decreases with the number of pillars and takes negative values for arrays with  $N > 50 \times 50$  pillars. We have also realised that our skewed data are correctly fitted by a three-parameter skew-normal distribution (SND) [22], [23] whose density function is defined by

$$SND(x) = \frac{\operatorname{erfc}\left(-\alpha \frac{x-\mu}{\sqrt{2}\sigma}\right)}{\sqrt{2\pi}\sigma} \exp\left[-\left(\frac{x-\mu}{\sqrt{2}\sigma}\right)^2\right] \quad (3)$$

Parameters  $\mu$ ,  $\sigma$  and  $\alpha$  are respectively: location, scale and shape parameters of the SND.

### III. RESULTS AND DISCUSSION

Applying the LLS rule, we mimic the loading process in two-dimensional square arrays with number of pillars ranging from  $N = 40 \times 40$  to  $N = 160 \times 160$ . We have simulated the strength of pillar-load-threshold non-homogeneity by changing values of the Weibull parameter  $k$ . Specifically, we have kept  $2 \leq k \leq 9$ . To achieve reliable estimates of  $Q_c$  and  $n_c$  each simulation was repeated at least  $10^4$

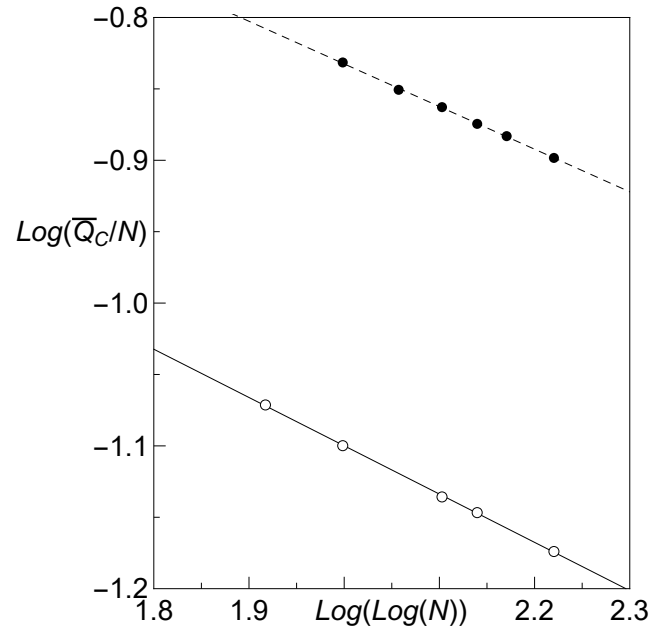


Fig. 2. Mean critical load  $\bar{Q}_c$  for arrays with growing number of pillars  $N$  and component-load-thresholds taken from the Weibull distribution with  $k = 2$  (open circles) and  $k = 4$  (black disks). Slopes of straight lines yield values of  $\delta$  in Eq. (4).

times (at least  $2 \times 10^3$  times for arrays with more than  $100 \times 100$  pillars). In such a framework we have collected large data sets containing detailed information about applied loads ( $Q$ ) and corresponding numbers of crushed pillars ( $n$ ). Analysing these  $Q$ 's and  $n$ 's data sets we have determined appropriate statistics by merging the both, critical load  $Q_c$  and corresponding number of intact components  $n_c$ , along with some empirical estimators as *e.g.* the mean values and the standard deviations.

#### Mean critical load

Under the computation method described above we have gathered long records containing critical loads  $Q_c$  as well as corresponding critical numbers of components  $n_c$ . Then, based on these records we have studied appropriate empirical probability density functions. In Fig. (2) we show how the mean critical load  $\bar{Q}_c$  depends on the number of pillars  $N$ , for different strengths of disorder, namely for  $k = 2$  (open circles) and  $k = 4$  (filled circles). Since for both the values of  $k$  the computed  $\log(\bar{Q}_c/N)$  are linearly dependent on  $\log(\log(N))$  then

$$\bar{Q}_c \sim \frac{N}{(\log(N))^\delta}, \quad (4)$$

where  $\delta$  is a function of  $k$ . For our chosen pair of  $k$  this exponent  $\delta$  equals to  $0.338 \pm 0.002$  and  $0.296 \pm 0.015$  for  $k = 2$  and  $k = 4$ , respectively.

Interestingly, for the same set of arrays, but with pillars' load thresholds  $\sigma_{th}$  distributed uniformly over  $[0, 1]$  the exponent  $\delta$  equals to 0.414 [24].

#### Critical number of pillars

Based on records related to  $n_c$  we have also analysed the resulting empirical probability density functions. Two of such

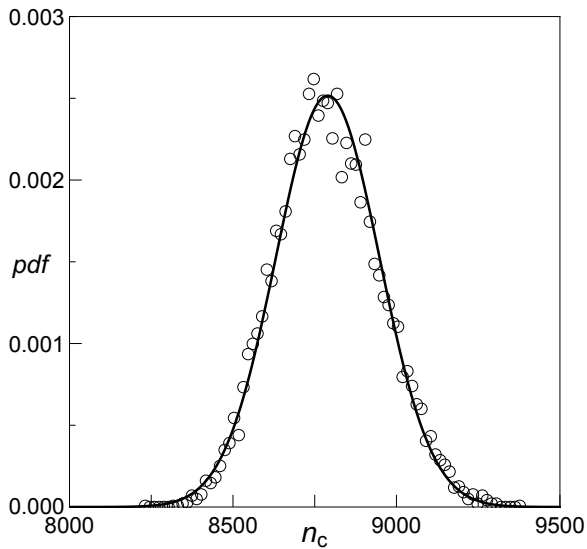


Fig. 3. Empirical probability density function (*pdf*) of  $n_c$  for systems with  $N = 100^2$  components with component-load-thresholds taken from the Weibull distribution with  $k = 2$ . The solid lines represent normally distributed  $n_c$  with the parameters computed from the simulations. The results are obtained from  $10^4$  samples.

empirical functions are presented in Fig. (3), for  $k = 2$ , and in Fig. (11b), for  $k = 4$ .

Analysis of all our experimental distributions of  $n_c$  enable us to fit these distributions by a normal distribution with a mean ( $\tilde{\mu}$ ) and a variance ( $\tilde{\sigma}$ ) that can be approximated by scaling relations:  $\tilde{\mu}(N, k) \sim N\mu(k)$  and  $\tilde{\sigma}(N, k) \sim N\sigma(k)$ . It turns out that the scaled mean can be written as

$$\mu(k) = 1 - \frac{a(N)}{k^{7/4}}, \quad (5)$$

where the coefficient  $a(N)$  depends on system size only and  $0 < a(N) < 1$  for all  $N > 50$ . The scaling (5) is presented in Fig. (4) for arrays with different number of pillars. The relative error ( $\tilde{\mu}/\mu - 1$ ) of this approximation lies in the interval  $(-0.002, 0.003)$ .

In the same way we have fitted values of  $\tilde{\sigma}$  by a function

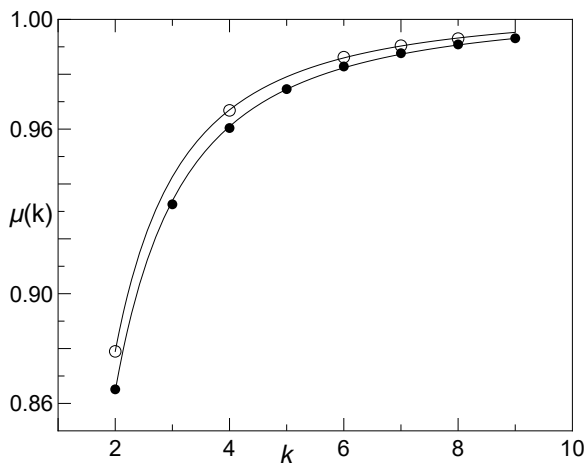


Fig. 4. Mean value  $\mu(k)$  of scaled critical number of pillars  $= n_c/N$  as a function of the Weibull shape parameter  $k$ . Arrays with  $N = 100 \times 100$  pillars - open disks, arrays with  $60 \times 60$  pillars - filled disks. The solid lines are drawn using (5).

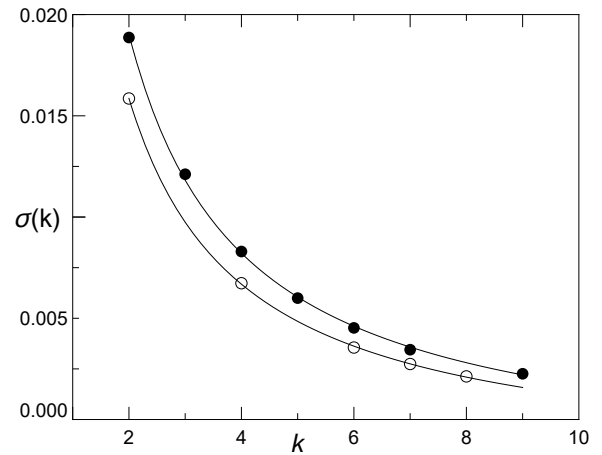


Fig. 5. Variance  $\sigma(k)$  of scaled critical number of pillars  $= n_c/N$  as a function of the Weibull shape parameter  $k$ . Arrays with  $N = 100 \times 100$  pillars - open disks, arrays with  $60 \times 60$  pillars - filled disks. The solid lines are drawn using (6).

$\sigma$  defined as:

$$\sigma(k) = \frac{b(N)}{k}, \quad (6)$$

where  $0 < b(N) < 1$  for  $N \gg 1$ . The computed standard deviation  $\tilde{\sigma}$  and the scaling (6) are displayed in the inset of Fig. (4). The relative error  $(\tilde{\sigma}/\sigma - 1)$  of this approximation lies in the interval  $(-0.034, 0.025)$  for all simulated systems. It is interesting to note that for arrays with pillar-load-threshold uniformly distributed over a segment  $[0, 1]$  and LLS transfer rule, the critical number of components is also normally distributed [25].

#### Local load intensities prior to catastrophic failure

Prior to destruction of the array, the applied load attains its maximal value  $Q_c$ , i.e. it is the maximal load that can be carried by the system. In the same time the array possesses a minimal number of pillars supporting  $Q_c$ . This means that  $Q_c/n_c$  represents an average intensity of imposed load. In a case when all working pillars equally share a load transferred from destroyed pillars, the load  $Q_c$  is composed from values of load-thresholds of the weakest pillars. However, within the LLS rule, that we consider in this work, only components that are neighbours of a failure suffer from an extra load. This means that the intensity of imposed load is not uniform throughout the array and ensemble of eliminated pillars does not contain the weakest pillars only. A closer look at gathered sets of  $Q_c$  and  $n_c$  yields that  $Q_c$  and  $n_c$  are strongly anti correlated, see Fig. (6). The Pearson coefficient ( $r$ ) computed from their distributions has values  $r \in (-0.96, -0.88)$  for all collected data. In Fig. (7) we present an example of an experimental joint probability distribution built by assembling, sample by sample, the critical load  $Q_c$  with the number  $n_c$  of components working under  $Q_c$ .

We start our analysis by comparing values of  $Q_c/n_c$  collected from two groups of arrays: (i) arrays with growing number of pillars while the strength of disorder is kept constant, i.e.  $N \neq const.$ ,  $k = const.$  and (ii) the number of pillars is fixed whereas the strength of disorder changes. Figures (8) and (9) show empirical probability density functions of  $Q_c/n_c$  for arrays of pillars representing (i) and (ii),

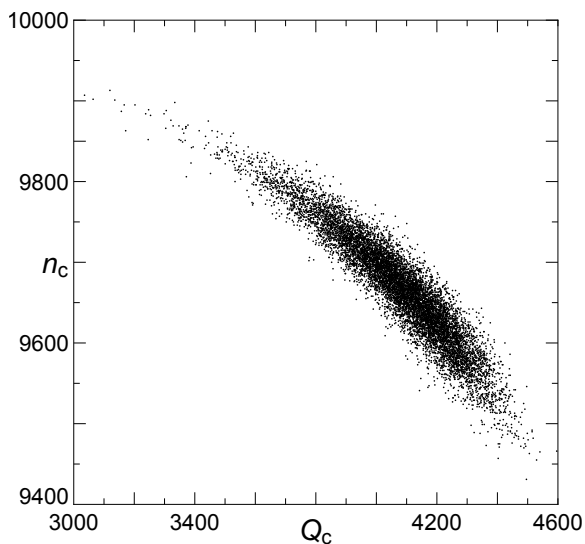


Fig. 6. Critical number of components  $n_c$  vs. critical load  $Q_c$  for systems with  $100^2$  components and load-thresholds drawn from the Weibull distribution with  $k = 4$ . Sample size is  $10^4$ .

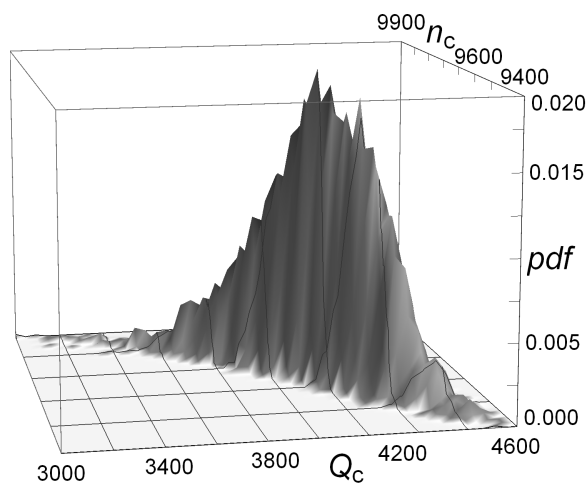


Fig. 7. Empirical joint probability density function of  $Q_c$  and  $n_c$  for arrays with  $100^2$  pillars and load-thresholds drawn from the Weibull distribution with  $k = 4$ . Sample size is  $10^4$ .

respectively. In Fig. (8), that corresponds to the case (i), the maximum of  $Q_c/n_c$  is pushed left for a growing number of pillars. This is because for growing  $N$  the number of relatively weak pillars also increases and this gives rise to a growing probability of subsequent failures. This is in contrast to the case (ii), presented in Fig. (9): increasing values of  $k$  reflect a decreasing variance of pillar-load-thresholds and, in consequence, arrays with higher values of  $Q_c/n_c$ .

A rigorous analysis of data presented in Figs. (8) and (9) reveals that the experimental distributions of  $Q_c/n_c$  have statistical properties described by the SND (3). In these plots we have added fitting lines of skew normal probability density functions with parameters computed from the samples. We also present a quantile-quantile (Q-Q) plot of the quantiles related to one of the collected data set against the corresponding quantiles given by the SND. As it is seen in Fig. (10), the points closely follow the straight line which indicates that the set of empirical data comes from the population with underlying skew normal probability distribution.

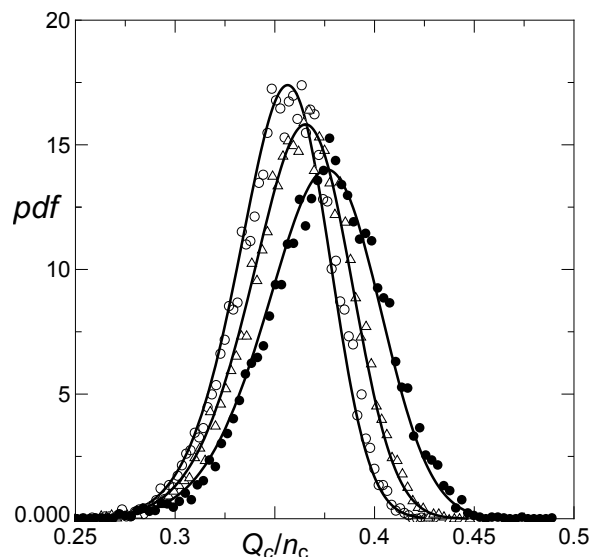


Fig. 8. Empirical probability density functions (*pdf*) of  $Q_c/n_c$  for arrays with  $N = 100^2$  (open circles),  $N = 80^2$  (triangles) and  $N = 60^2$  (filled circles) pillars. Pillar-load-thresholds are governed by the Weibull distribution with  $k = 2$  for all presented arrays. The solid lines represent skew-normally distributed  $Q_c/n_c$  with the parameters computed from the simulations. The results are obtained from at least  $10^4$  samples for each value of  $N$ .

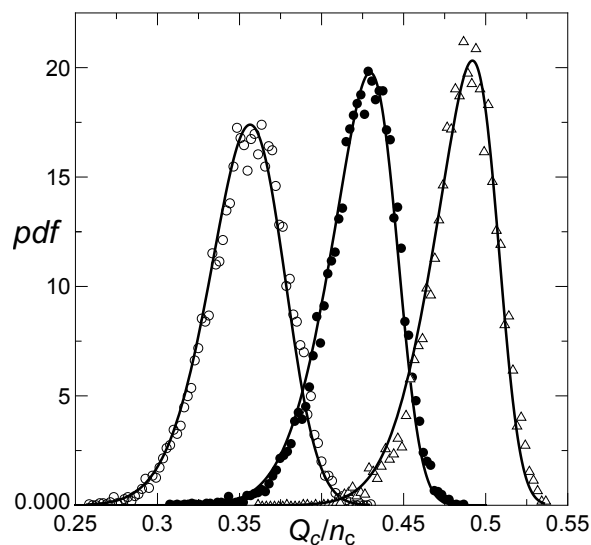


Fig. 9. Empirical probability density functions (*pdf*) of  $Q_c/n_c$  for systems with  $100^2$  components and load-thresholds drawn from the Weibull distribution:  $k = 2$  (open circles),  $k = 4$  (filled circles) and  $k = 6$  (triangles). The solid lines represent skew-normally distributed  $Q_c/n_c$  with the parameters computed from the simulations. The results are obtained from  $10^4$  samples for each value of  $k$ .

Beside the fact, that we display this Q-Q plot only for an estimate purpose, we have examined our simulated data sets using different goodness of fit tests. We have also estimated values of the location, scale and shape parameters of the SND by employing the maximum likelihood procedure.

We finalize our analysis of quantities, that represent arrays of vertical pillars on their edge of functionality, with an example of the array whose  $100 \times 100$  component-load-thresholds are characterized by the Weibull shape parameter  $k = 4$ . This array is sufficiently large, with still moderate disorder, to be representative for arrays studied in this

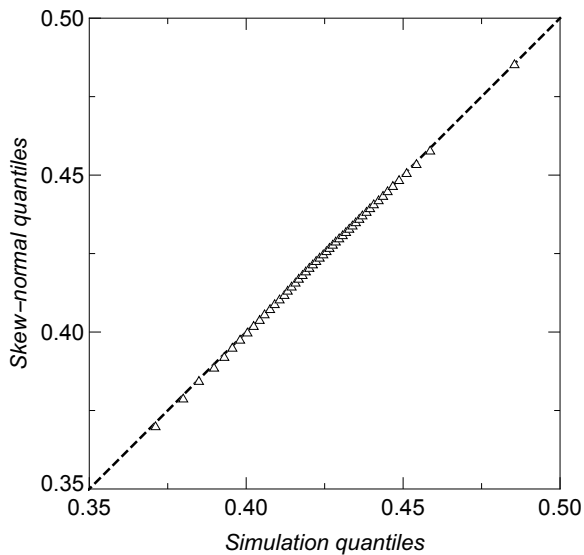


Fig. 10. Quantile-Quantile plot of the quantiles of the set of computed  $Q_c/n_c$  vs. the quantiles of the skew normal probability distribution for arrays with  $100 \times 100$  pillars and load-thresholds taken from the Weibull distribution with  $k = 4$ . Sample size is  $10^4$ .

work. In Fig. (11) we present experimental distributions of quantities collected during simulations carried out with this arrays of pillars, i.e. distributions of:  $n_c$ ,  $Q_c$ ,  $Q_c/n_c$  as well as  $Q_c$  vs.  $n_c$ . We have already mentioned that the experimental distribution of  $Q_c$ , presented in Fig. (11a) can be fitted correctly by the Weibull distribution [21]. Also Figs. (6) and (7) are related to this array, namely they show the experimental joint probability distribution of  $Q_c$  and  $n_c$ .

#### IV. SUMMARY

In this paper we have analysed statistics of failures in progressively loaded arrays of pillars. We considered sets of compressed vertical nano-sized pillars placed in nodes of a square array. Pillars' imperfections are modelled by quench random load-thresholds governed the Weibull probability distribution. Based on results of simulations, collected under the LLS rule, we conclude that the experimental distributions of the critical load  $Q_c$ , critical number of pillars  $n_c$  as well as the local-load intensity  $Q_c/n_c$  can be effectively estimated. By fitting discrete distributions we have found that prior to catastrophic destruction: (i) the ratio  $Q_c/n_c$  is skew-normally distributed, (ii) the number of working pillars is normally distributed and (iii) for  $N \gg 1$ , the mean and variance of normally distributed  $n_c/N$  scale like  $(1 - \mu/N) \sim 1/k^{7/4}$  and  $\sigma \sim 1/k$ , respectively, (iv) for large values of  $N$  the mean value  $\bar{Q}_c$  diverges as  $N/(\log(N))^\delta$ , with  $0 < \delta < 1$ .

#### REFERENCES

- [1] J.R. Greer, D. Jang, J.-Y. Kim, J. Burek, "Emergence of New Mechanical Functionality in Material via Size Reduction," *Adv. Functional Materials*, vol. 19, pp. 2880–2886, Sept. 2009.
- [2] P. Sievila, N. Chekurov, I. Tittonen, "The fabrication of silicon nanostructures by focused-ion-beam implantation and TMAH wet etching," *Nanotechnology*, vol. 21, id. 145301, March 2010.
- [3] N. Chekurov, K. Grigoros, A. Peltonen, S. Franssila, I. Tittonen, "The fabrication of silicon nanostructures by local gallium implantation and cryogenic deep reactive ion etching," *Nanotechnology*, vol. 20, id. 065307, Feb. 2009.

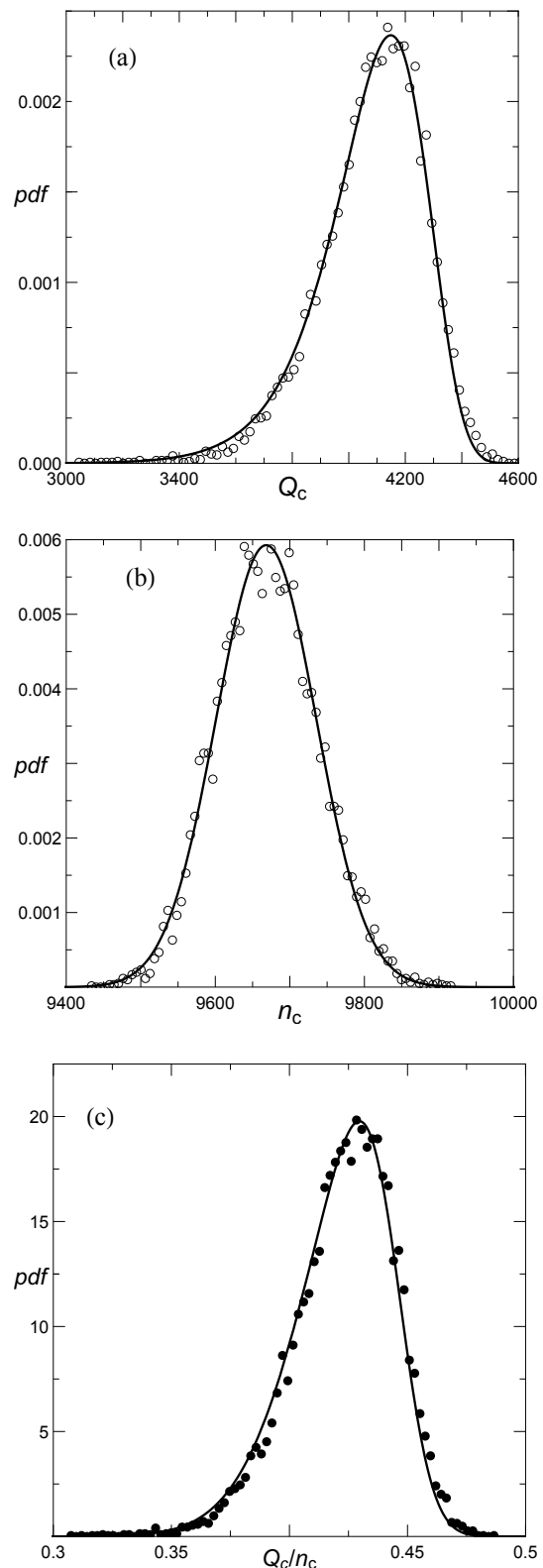


Fig. 11. Empirical probability density functions (*pdf*): (a) critical load  $Q_c$ , (b) critical number of pillars  $n_c$  and (c) ratio  $Q_c/n_c$ . Arrays involve  $N = 100 \times 100$  pillars and pillar-load-thresholds are taken from the Weibull distribution with  $k = 4$ . The solid lines represent fitted distributions: (a) Weibull, (b) normal (c) skew-normal, with the parameters computed from the simulations. Presented results are evaluated from  $10^4$  samples.

- [4] D. Jang, J.R. Greer, "Transition from a strong-yet-brittle to a stronger-and-ductile state by size reduction of metallic glasses," *Nature Materials*, vol. 9, pp. 215–219, Feb. 2010.
- [5] C. Manzato, A. Shekhawat, P. K. V. V. Nukala, M. J. Alava, J. P. Sethna, and S. Zapperi, "Fracture Strength of Disorder Media: Universality, Interactions, and Tail Asymptotics," *Phys. Rev. Lett.*, vol. 108, id. 065504, Feb. 2012.
- [6] Z. Bertalan, A. Shekhawat, J.P. Sethna, and S. Zapperi, "Fracture strength: Stress concentration, extreme value statistics and the fate of the Weibull distribution," *Phys. Rev. Applied*, vol. 2, id. 034008, Sept. 2014.
- [7] S. Zapperi, P. Ray, H.E. Stanley, and A. Vespignani, "Analysis of damage clusters in fracture processes," *Phys. A*, vol. 270, pp. 57-62, Aug. 1999.
- [8] Z. Domański, "Simulation Study of Failures in Progressively Loaded Multicomponent Systems," *Lecture Notes in Engineering and Computer Science: Proceedings of The World Congress on Engineering and Computer Science 2017*, 25-27 October, 2017, San Francisco, USA, pp. 742-746.
- [9] D. Sornette, "Elasticity and failure of a set of elements loaded in parallel," *J. of Physics A: Mathematical and General*, vol. 22, No. 6, pp. L243-L251, March 1989.
- [10] A. Hansen, P.C. Hemmer, and S. Pradhan, "The Fiber Bundle Model: Modeling Failure in Materials," Weinheim, Wiley-VCH, 2015.
- [11] S. Pradhan, A. Hansen A., and B.K. Chakrabarti, "Failure processes in elastic fiber bundles," *Rev. Mod. Phys.*, vol. 82, pp. 499-555, March 2010.
- [12] M.J. Alava, P.K.V.V. Nukala, and S. Zapperi, "Statistical models of fracture," *Adv. In Physics*, vol. 55, pp. 349-476, April 2006.
- [13] F. Kun, F. Raischel, R.C. Hidalgo, and H.J. Herrmann, "Extensions of fibre bundle models," in *Modelling Critical and Catastrophic Phenomena in Geoscience, Lecture Notes in Physics*, P. Bhattacharyya and B.K. Chakrabarti, Eds, vol. 705, Berlin: Springer 2006, pp. 57-92.
- [14] R.C. Hidalgo, Y. Moreno, F. Kun, and H.J. Herrmann, "Fracture model with variable range of interaction," *Phys. Rev. E*, vol. 65, id. 046148, April 2002.
- [15] R.C. Hidalgo, S. Zapperi, and H.J. Herrmann, "Discrete fracture model with anisotropic load sharing," *J. Stat. Mech.*, id. P01004, Jan. 2008.
- [16] T. Derda, "Analysis of damage processes in nanopillar arrays with hierarchical load transfer," *J. Appl. Math. Comput. Mech.*, vol. 15(3), pp. 27-36, 2016.
- [17] F. Raischel, F. Kun, and H.J. Herrmann, "A simple beam model for the shear failure of interfaces," *Phys. Rev. E*, vol. 72, id. 046126, Oct. 2005.
- [18] J. Knudsen and A.R. Massih, "Breakdown of disordered media by surface loads," *Phys. Rev. E*, vol. 72, id. 036129, Sept. 2005.
- [19] W. Weibull, "A statistical distribution function of wide applicability," *J. Appl. Mech.*, vol. 18, pp. 293-297, Sept. 1951.
- [20] N.M. Pugno and R.S. Ruoff, "Nanoscale Weibull statistics," *J. Appl. Phys.*, vol. 99, id. 024301, Jan. 2006.
- [21] Z. Domański and T. Derda, "Distribution of critical load in arrays of nanopillars," *Lecture Notes in Engineering and Computer Science: Proceedings of The World Congress on Engineering 2017*, 5-7 July, 2017, London, UK, pp. 797-801.
- [22] A. Azzalini and A.R. Massih, "A class of distributions which includes the normal ones," *Scand. J. Statist.*, vol. 12, pp. 171-178, June 1985.
- [23] A. Azzalini, "The Skew-Normal and Related Families," Cambridge: Cambridge University Press, 2013.
- [24] Z. Domański, T. Derda, and N. Sczygiol, "Critical avalanches in Fiber Bundle Models of Arrays of Nanopillars," *Lecture Notes in Engineering and Computer Science: Proceedings of International Multiconference of Engineers and Computer Scientists 2013*, March 13-15, 2013, Hong Kong, pp. 765–768.
- [25] "Statistics of critical avalanches in vertical nanopillar arrays," in *Transactions on Engineering Technologies. Lecture Notes in Electrical Engineering*, G.C. Yang, S.I. Ao, X. Huang, O. Castillo, Eds., vol. 275, Dordrecht: Springer, 2013, pp. 1-11.